Ancient TL

www.ancienttl.org · ISSN: 2693-0935

Issue 17(2) - December 1999
https://doi.org/10.26034/la.atl.v17.i2

# The ROSY ESR dating program

B. J. Brennan*, W. J. Rink†, E. M. Rule†, H. P. Schwarcz† and W. V. Prestwich‡

*Department of Physics, The University of Auckland, New Zealand
†School of Geography and Geology, McMaster University, Hamilton, Ontario, Canada
‡Department of Physics, McMaster University, Hamilton, Ontario, Canada

*(Received 18 April 1999; in final form 18 August 1999)*

***Abstract :*** *ROSY is a program that enables the calculation of average dose rates and age estimates in the ESR dating of tooth enamel, but has more general applicability to other situations involving layers of different media in planar geometry. The user has the freedom to change a wide range of parameters, including the composition of each of the media. The latest Version, 1.4, includes consideration of gradients in the alpha track dose as well as in the beta dose, and several options for the input or computation of gamma and cosmic ray doses. The theoretical assumptions and procedures used in the ROSY calculations are described. We discuss the various user-controllable features of the program and the input and output of data, and aspects that may need particular attention by users are highlighted. Possible improvements to the software in future Versions are discussed.*

## 1 Introduction

ROSY is a program that enables the calculation of dose rates and age estimates for a planar geometry involving up to three layers embedded in an infinite matrix. It is named after a hippopotamus which died at the Toronto Zoo and posthumously lost her teeth to the cause of ESR dating at McMaster University Geology Department. While the program employs terminology specific to the ESR dating of tooth enamel, it may be adapted readily to other situations in luminescence or ESR dating where the geometry is essentially planar for the purpose of beta dose calculations, such as mollusc shells and thin burned flints. The primary purpose of the present paper is to outline the various user-controllable features and the methodology employed in ROSY and to comment on aspects that may need to be considered by a user. This includes coverage of improvements made to the software since a brief summary of the program was previously presented (Brennan *et al.*, 1997). Not all the features discussed are implemented in versions of ROSY earlier than the current version, 1.4.

The most significant feature of ROSY is the use of "one-group" theory in the calculation of beta dose contributions, and this aspect has been discussed elsewhere. Brennan *et al.* (1997) describe the formalism and present comparisons of ROSY beta dose estimates with estimates from the DATA software based on the approach of Grün (1986), theoretical Monte Carlo results, and the experimental results of Aitken *et al.* (1985). These comparisons revealed significant differences, with ROSY and the Monte Carlo results in broad agreement but yielding lower doses than either DATA or Aitken *et al.* (1985). Yang *et al.* (1998) conducted careful experiments to measure beta attenuation in planar dose geometry, and these produced results in substantial agreement with one-group and Monte Carlo calculations. As a consequence, we believe that the ROSY software provides better estimates of the beta dose (and hence of the total dose) to a layer than previous software.

It is arguable that modern Monte Carlo-based data would be more accurate again, as has been suggested (Grün, 1998). The rationale for applying the one-group theory arose from its suitability in accounting for layered geometry, in particular the effect of back-scattering at boundaries. This simplified model leads to an exponential behavior for the dose attenuation resulting from external irradiation from each side. It should be emphasised that it is an experimentally established fact that the dose distribution for a given beta emitter is not exponential. As a consequence, no unique attenuation coefficient exists and any effective attenuation coefficient representing the actual distribution would vary with the range over which the distribution is being approximated. The concordance of results based on the use of one-group attenuation coefficients with Monte Carlo calculations and the results of Yang *et al.* (1998) is thus probably

fortuitous. Work is currently in preparation incorporating into ROSY the use of Monte Carlo-based data in place of one-group theory for estimating beta doses (Marsh, 1999).

Version 1.4 of ROSY allows for alpha dose variation near the boundaries of the enamel layer, whereas previous versions simply used the "infinite matrix" dose rate for the enamel. Proper allowance for such alpha dose gradients is necessary in dating thin enamel or mollusc layers where stripping of boundary material is not appropriate.

## 2 Layered Geometries in ROSY

ROSY can calculate the dose for tooth enamel in a range of environments and solve for the age consistent with the observed equivalent dose, $D_E$, using different uranium uptake models for the enamel, cementum, and dentine tissues. In calculating the beta and alpha doses to the enamel "target" dose absorber, ROSY makes the assumption that all layers (enamel, sediment, cementum, and dentine) are homogeneous, planar, and parallel. The dose includes an internal component due to sources within the enamel and an external component due to sources in other layers. The most complex geometry that ROSY can work with consists of a layer of enamel sandwiched between cementum and dentine in surrounding sediments (Figure 1).

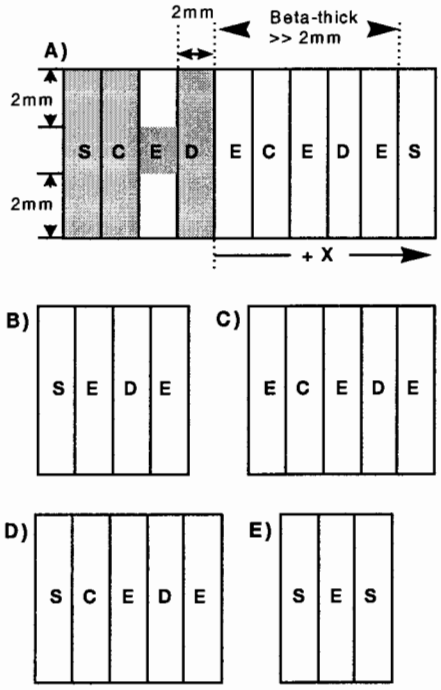


***Figure 1.*** *Beta dose geometry of tooth enamel layers.*

*A) Cross-sectional view of one possible sequence of layers in a bovid or cervid tooth showing cementum (C), enamel (E) and dentine (D) surrounded by sediment (S) on both sides. The enamel portion for dating (shaded in Figure 1A) should be adjacent to a dentine layer that is at least 2 mm thick, and C, E, D should all be located in planar layers that extend for 2mm beyond the enamel edges. This insures proper 2* $\pi$ *geometry for beta irradiation. In most cases, the internal layering labelled beta-thick (and the dentine adjacent to the enamel if present) will shield the dated enamel from beta irradiation by the sediment layer on the positive X side (diagram right). The ROSY calculation will include a beta contribution from sediment on this side if too small a value is entered for the thickness of the "dentine" layer.*

*Four cases of actual geometries which can be used in ROSY:*

*B)* ***SED:*** *Outer enamel layer that occurs between sediment and dentine.*
*C)* ***CED:*** *Inner enamel layer that occurs between cementum and dentine.*
*D)* ***SCED:*** *Outer enamel layer that lies between cementum and dentine.*
*E)* ***SES:*** *Enamel detached from tooth and surrounded completely by sediment.*

The geometry of layers in mammal teeth depends on taxon. Figure 1 is a schematic diagram showing the arrangement of layers seen in a transect across a bovid or cervid tooth (horse teeth can have as many as 25 different layers across a single transect). Although the layers are idealised as true planar layers in Fig. 1, in real situations the outer enamel layers are generally more planar, albeit slightly curved, while the inner layers of enamel are more convoluted. Workers may choose to use the outer enamel layers or inner enamel layers, but some simple rules about geometry are important. As Figure 1A shows, the ideal enamel section for dating should come from a region where the layers are nearly planar (slightly curved layers are a good approximation to planar geometry). In addition, the layers adjacent to the enamel should extend some 2mm laterally beyond the dated portion, so that edge effects which disrupt planar irradiation geometry during burial can be avoided. The 2mm maximum range of most of the beta particles controls this dimension. In addition, when the inner tooth layers are beta-thick (that is, greater than the 2mm maximum range of natural beta particles), they shield the enamel from any beta dose being delivered by the sediment in the region X>0 in Figure 1A. ROSY software calculations always include a beta dose contribution from the sediment in the region X>0 (on the right of each diagram) unless the thickness of dentine entered into the program is at least 2000 micrometer (2mm). Sediment "layers" are always assumed to be infinitely thick for the purpose of beta dose calculations.

There are four general cases to which ROSY is applicable, which include most if not all configurations of dental layers found in nature. These are summarised in Figures 1B-E. In both the caption and the discussion which follows, the labels used list in left-to-right order the layers in each geometric configuration which contribute the bulk of the beta dose to the enamel.

**SED** (Figure 1B): Cementum thickness is zero, as no cementum is present on the external surface of the enamel.

**CED** (Figure 1C): Both C and D are beta-thick; this configuration could represent an inner enamel layer of a hypsodont tooth, where typically the enamel is bordered by cementum and dentine. If either C or D are not beta-thick (> 2 mm) then some beta dose from adjacent E must be included (see discussion below). Use of a layer thickness significantly larger than 2 mm for input into ROSY can result in minor variations (at the 1% level) in the beta doses calculated by ROSY, arising from numerical roundoff errors and approximations in the calculation algorithm when very thick layers are involved.

**SCED** (Figure 1D): A beta-thin C layer is external to E. This layer acts as a partial absorber of beta particles from S, and also generates a beta dose which is computed by ROSY from its U concentration and thickness.

**SES** (Figure 1E): A special case in which the enamel has been completely isolated from the other layers of the tooth. For age calculations one must assume this has been true for virtually all of the burial history. In this case, with the thicknesses of both the C and D layers being zero, the sediments provide the entire external beta dose.

Data input is more complex for cases where internal dentine layers (such as those in Figs. 1B, C, D) or an internal cementum layer (as in Fig. 1C) are not a full 2mm thick. In these cases, the actual sources of external beta dose to the dated enamel are in a set of multiple tissue layers such as cementum (or dentine) plus the next nearest neighbour enamel layer. Here the problem is that ROSY input needs to reflect the fact that the C+E or D+E layer of approximately 2mm thickness has a mixed composition.

The soundest approach is to use ROSY to model an interior sequence such as $E_1CE_2DE_3$ (with the $E_2$ layer being dated) by using the five layers in a ROSY SCEDS sequence and replacing the "sediment" parameters with parameters appropriate to the layers $E_1$ and $E_3$. This requires the assigned parameters of those two enamel layers to be identical, and a gamma dose rate now has to be entered separately into ROSY (as the sediment source concentrations are no longer available for use). If the combined thickness of $E_1C$ or $DE_3$ is not beta-thick, then even this approach will be approximate.

A less satisfactory approach would be to input parameters for the C and D layers in ROSY which reflect averages for any composite C+E or D+E layers. However, if the C and/or D layers in the composite layers are U-rich, simple averaging of the bulk composition of the composite layer would not reflect the fact that the largest part of the beta dose received by the enamel emanates from the portion nearest the enamel. If a C or D layer is at least one mm thick, treating the composite layer as if it were fully C or D would be more accurate than using a simple average.

Alpha radiation doses from the external radiation sources (and also the gradient in the internal alpha dose near the edges of the enamel) can be removed by stripping a thin layer off each side of the enamel. Stripping of at least 40 micrometer from each side is recommended to accomplish this.

While the terminology used for the layers in ROSY is specific to the context of dating tooth enamel, the approach is valid for any geometrically similar problem involving adjacent planar homogeneous layers of different materials. ROSY can be used in such situations by simply assigning new meanings to the built-in titles "sediment", "cementum", "enamel", and "dentine", as in the discussion for internal layers above, and adjusting the compositions of media accordingly.

## 3. Data input

For the range of environments discussed above, ROSY calculates the dose to the stripped tooth enamel layer, and solves for the age consistent with the observed $D_E$ using different uptake models. The compositions (including water content) of all media and the thicknesses of the enamel, cementum and dentine layers may be varied. Age estimates are calculated assuming early and linear U uptake (see, for instance, Grün *et al.*, 1987) in all tooth tissues, and also for a user-changeable combination in which either early or linear uptake may be chosen separately for each tooth tissue. The defaults for this combination are early uptake in enamel and linear uptake in dentine and cementum.

ROSY gives the user the options of reading input data from a file or using default data and it is then possible to make changes to these data. The first menu screen, a typical example of which is shown in Figure 2, displays and handles changes for various parameters (and their errors where appropriate). The parameters on this screen include those defining the geometry, water composition, and radioactive source concentrations for all media, other data relating to the dosimetry, and parameters specific to the enamel material used as a dosimeter.

Since the program is written in FORTRAN 77 for an MS-DOS screen, the screen interaction is not sophisticated, but an easy sequence of mainly letter-based keystrokes and returns invokes appropriate prompts, enabling straightforward alteration of any parameter or its error. The parameters are displayed in lines on the screen and parameters on each line may be altered on entering the alphabetic character at the left of that line. Prompts and messages appear at the bottom of the screen. The input screen is then updated to await requests for any further changes. It is intended that reading the prompts and messages will provide a self-explanatory route through the program, so that a detailed user instruction manual is not required. Explanatory comments relating to some of the parameters follow.

Concentrations of radioelements in sediment or tooth are given as ppm U, Th, and weight percent K, as fractions of the dry material. The density of the dental tissues and sediment can be user-defined. The default values of density for enamel, cementum and dentine are the average values found by Rink and Hunter (1998) for fossil teeth.

The assumptions and methodology used in alpha dose calculations are detailed in the section on dose calculations. The input value for alpha efficiency is taken to be the $k$ value for the entire track length of an alpha particle at reference energy 5.3 MeV, which was the alpha energy used by de Canniere *et al.* (1986) in obtaining a $k$ value of 0.15 for tooth enamel.

Four options are available for gamma and cosmic ray dose rates in ROSY Version 1.4:

1) The combined total dose rate may be specified;
2) the gamma dose rate may be specified, with the cosmic dose rate being calculated by ROSY using input values for depth and density of overburden;
3) the cosmic dose rate may be specified, with the gamma dose rate being calculated by ROSY using the sediment U, Th and K concentrations for the latter; and
4) the user may request ROSY to calculate both the cosmic ray and gamma dose rates.

Figure 2 shows an example using the second of these options. Note that if the sediment concentration values used are atypical and reflect only the material within about 2mm of the tooth (for the purpose of accurate beta dose calculations), a value for gamma dose will need to be supplied. In other situations, allowance may need to be made for the presence of significant quantities of non-sedimentary material around the dated material. This can modify the sediment infinite-matrix gamma dose rate (see Rink *et al.*, 1996, for an example involving an elephant tooth encased in a mandible).

A second menu screen prompts in a similar fashion for changes to the 'dry' composition by weight of each medium, using a limited range of elements (H, C, N, O, Na, Mg, Al, Si, P, S, Cl, K, Ca, Fe, Zn). The starting compositions are those read in from the input file, or default compositions if no input file is used. On exit from this second menu screen, ROSY revises the composition of each medium including the water content specified on the first menu screen.

This water content may be specified as a percentage of the dry mass of the medium or of the mass of the wet medium.

Since these compositions are used exclusively for computing interaction cross-sections and/or ranges, there is freedom on the second menu screen to group elements with similar atomic masses in representing the composition. Consistent with this approach, note that the content of (natural) potassium entered in the first menu screen, used to calculate K-40 activity, and the potassium content entered for a medium in the second menu screen do not have to be identical.

```
**********************************************************ROSY VER 1.4 ******
N            NAME OF FILE:    trial    .DAT
Q    EQUIVALENT DOSE [Gy]:      268.45     6.39
C              CALCULATING:        Ages
R   RATIO OF U234 TO U238:         1.40     0.00   Initial Ratio
A   ALPHA EFFICIENCY: 0.15     0.00   Varies with energy, Eref=5.3MeV
                           SEDIMENT       CEMENTUM         ENAMEL         DENTINE
U   U              [ppm]    8.15  0.10     0.00  0.00     0.00  0.00    21.20  0.10
T   TH             [ppm]    3.59  0.20     0.00  0.00     0.00  0.00     0.00  0.00
K   K              [wt%]    0.16  0.01     0.00  0.00     0.00  0.00     0.00  0.00
D   DENSITY      [g/cc]     2.00  0.10     2.52  0.25     2.95  0.00     2.78  0.28
F   FR. OF RADON            1.00  0.00     1.00  0.00     1.00  0.00     1.00  0.00
W   % WATER       (Dry)   15.00 10.00     5.00  0.00     0.00  0.00     5.00  0.00
H   THICKNESS [microns]       --            0.     0.     839.   151.   2000.     0.
P   UPTAKE 1=EARLY/2=LINEAR                    2              1              2
O   ENAMEL STRIPPED FROM OUTSIDE [microns]:      70.00    35.00
I   ENAMEL STRIPPED FROM INSIDE  [microns]:      40.00    20.00
G   GAMMA DOSE                 [microGy/year]:   358.00    81.00
G   DEPTH & DENSITY FOR COSMIC  [m & g/cc]:      10.00     0.00       2.13  0.00
**************************************************** ROSY VER 1.4 ******
Please enter the letter corresponding to the parameter you want to change.
To change an error value, type E, press return and enter the letter corresponding to the error you want to change.
If you enter any other character, this data will be used for calculations.
```

***Figure 2.*** *A typical example of the first menu screen for data input to ROSY, Version 1.4. All relevant parameters apart from the media compositions are changed using this screen. The format of the line(s) labeled "G" varies with the option selected by the user.*

## 4 Data output:

Once changes to compositions are complete, the user is given the option when calculating age estimates of including the error estimate. The computation time is then a little longer, but with a Pentium CPU the time penalty is negligible.

When ROSY is used to calculate ages (the usual mode), the results for each uptake model in the output file consist of the calculated dose (equal to the equivalent dose), the age estimate and its error estimate, a table showing a breakdown of average dose rates, the average (alpha plus beta) dose rate, and the average total dose rate. The table lists average annual dose rate components by type (alpha, beta, gamma, cosmic), and, where appropriate within each type, by source medium (enamel, cementum, dentine, sediment) and by radiation parent (U, Th, K, total). A briefer summary is written to the screen.

The user is allowed to calculate either the ages consistent with the equivalent dose for each uptake model ('Ages' option) or the dose rates for specified ages ('Dose rates' option). It would be usual to use

the 'Ages' option, but the 'Dose rates' option can be useful to make comparisons (e.g., with other age algorithms) or to test variation of any component of the dose with time.

## 5 Dose calculations

Version 1.4 uses the data of Adamiec and Aitken (1998) on half-lives, energies, and branching ratios as the primary data for ROSY calculations. By comparison with the previously used data of Nambi and Aitken (1986), the most significant adjustments to infinite matrix dose rates, all downwards, occur for beta and gamma doses from the Th-232 series (-4.4% and -8.3%) and for beta doses from K-40 (-4.1%). In the specific context of dating tooth enamel, these are rarely major contributors to the total average dose rate, and the effect on an age estimate is not likely to exceed 2%.

Age estimates for each uptake model are obtained by finding the zero in the difference between the calculated total dose and the input equivalent dose as a function of time. For a given trial age and uptake model, ROSY first computes the total number of decay events per unit volume for each radioactive source in each medium. This computation allows for changes in U concentration associated with the style of uptake in D, C, and E (but not in S) and for the corresponding changes in activity as a result of approach of the U-series isotopes to secular radioactive equilibrium (as in Grün *et al.*, 1987). The decay event densities are then used to calculate the average total dose at the trial age to the enamel remaining after stripping. Using standard numerical techniques, the trial age is varied until the calculated dose matches the equivalent dose to within one part in a million.

At the completion of each age estimate, ROSY checks the implied initial ratio for the activities of U-234 and U-238 in the tooth tissues (a constant ratio of unity is assumed for the sediments). If this ratio is less than 0.6 or greater than 8.0, the initial ratio is set equal to 0.6 or 8.0 as appropriate, the age is calculated on that basis, and an error message is printed warning that the age estimate is invalid. For older samples, such unrealistic ratios can result when the user selects the option to specify the present activity ratio and this is then extrapolated back in time using the uptake model in question. Specification of the initial ratio or of a present ratio closer to unity may be required to yield a 'valid' age. If the present ratio used is based on sample data, the invalid age may reflect fluctuations in uranium mobility and uptake over the age of the sample which cannot be modelled accurately with ROSY.

### Alpha dose

Version 1.4 of ROSY calculates the effective alpha dose on the assumption that the alpha-induced signal is proportional to the *track-dose*, that is, to the deposited *effective track length* per unit volume. The calculation uses an algorithm based on the approach of Aitken (1987) to model the gradient in track dose near a boundary of the enamel layer. This approach is accurate where the amount stripped off each side of the enamel is small or zero, and yields the expected infinite matrix dose when more than 40 micrometer is stripped off each side.

The effective track length is less than the actual track length because the final portion of an alpha track ($AT_F$) yields very little signal, despite the large amount of energy deposited on average in this ineffective portion of the track. In ROSY calculations, the effective track length of an individual alpha particle (in units of density times distance) is set equal to the actual track length minus a proxy value of $AT_F$ (0.875 mg cm$^{-2}$), which is the experimental value of Lyons and Brennan (1989) for ESR in calcite. No direct measurement of $AT_F$ for tooth enamel is available. As mentioned above, the input value to ROSY for alpha efficiency is the *k* value for the entire track length of a 5.3 MeV alpha particle. Alphas of this energy coincidentally have an effective track length which is almost exactly the average value for alphas from natural uranium. Because track dose is used in the calculation, the *k* value for an individual alpha depends on the alpha energy

TRIM data (Ziegler *et al.*, 1985) for the ranges of the natural and reference alpha energies in the elements are incorporated in ROSY, and the specified elemental compositions of the materials are used to estimate the ranges of these alphas for each material. For each alpha energy, the reciprocal of the range in each element is taken as a proxy for the average stopping power for that element, and the range in the material is obtained by computing the weighted sum of these proxies and then taking the reciprocal of that sum. This straightforward technique copes with arbitrary variations in the compositions of all materials, but it is approximate, being exact only if the variation of stopping power with energy is of the same form for all elements. However, comparison with TRIM results for a range of feasible compositions indicates that the ROSY range estimates

are accurate to at worst 1%. The consequent error in the alpha dose to a layer would be dwarfed by other uncertainties, such as in the alpha effectiveness.

The alpha dose to the enamel remaining after any stripping is then calculated using the approach of Aitken (1987). However, as opposed to Aitken (1987), we use the effective track length in place of the track length itself. In effect, the track dose is the enamel infinite matrix dose rate, less any track dose deficit resulting from the escape of internal alpha particles, and plus any track dose deposited in the enamel from external sources. Grün (1987) applied Aitken's original formulation in a similar fashion to the external alpha irradiation of a calcite layer.

It is straightforward to show that equations such as (3), (4) and (6) of Aitken (1987) apply also where an inert layer is irradiated by alpha sources in an adjacent but different medium. The assumptions of these results are that the alpha-induced signal is proportional to the deposited effective track length, that all alpha tracks are straight, and that the ratio of the ranges of an alpha particle in the two adjacent media is a constant independent of the alpha energy. Departures from these assumptions in practice are not expected to result in large errors in the alpha dose estimate for the layer.

**Beta dose**

The mathematical basis for the application of one-group theory to beta dosimetry near planar interfaces is summarised in Prestwich *et al.* (1997), and briefer qualitative descriptions are to be found in Yang *et al.* (1998) and Brennan *et al.* (1997). The reader is referred to these papers for detail. In applying one-group theory, which was originally developed for modelling neutron transport, the complex interaction with media of betas from the spectrum of a beta emitter is modelled by considering a single group of electrons all with the mean energy. These interact via a combination of isotropic elastic scattering and complete absorption of part of each beam. The absorption cross section is taken to be the ratio of the stopping power to energy, evaluated at the average energy, and the scattering cross section is taken to be the Lewis transport cross section. Boundary conditions are imposed at interfaces to ensure continuity of electron flux in each direction. The theory shows reasonable agreement with experimental data on beta dose gradients in planar geometry (O'Brien *et al.*, 1964 and Yang *et al.*, 1997) and with theoretical results based on Monte Carlo simulations (Brennan *et al.*, 1997).

The work of Brennan *et al.* (1997) and Yang *et al.* (1998) shows that the approach based on one-group theory yields better estimates of average beta doses than other software used in ESR and TL dating for planar geometry. However, as mentioned in the introduction, the theory is based on *ad hoc* and entirely hypothetical assumptions and the results are necessarily approximate. For these reasons, use of Monte Carlo-based data would be preferable and the complex process of properly incorporating such data in a future version of ROSY is proceeding.

**Gamma and cosmic ray doses**

When calculating the gamma dose from the sediment source concentrations, ROSY estimates the infinite matrix gamma dose rate using the data of Adamiec and Aitken (1998). The estimate includes the factor given by Equation (4.7) of Aitken (1985), which allows for the enhanced mass absorption coefficient of the hydrogen-rich water. Situations where this infinite matrix estimate may not be appropriate have been mentioned in the previous section.

For cosmic dose rates, version 1.4 of ROSY uses equation (2) of Prescott and Hutton (1994) with the addition of a term that approximates the 'soft' component of the cosmic dose for very shallow burial depths. However, it should be noted that the formula used assumes level terrain at sea level and a latitude of 55°. Users may prefer to input their own cosmic ray dose rate estimate to ROSY. Graphs of parameters used in adjusting for latitude and altitude are displayed in Figure 2 of Prescott and Hutton (1994).

**Error estimates**

Errors in age estimates are calculated on the assumptions that the errors in individual parameters are independent of one another and that the input errors in parameters represent symmetric random errors and are estimates of standard deviation. Each input parameter is varied up and down by one standard deviation, the age estimate is recalculated and the variation is used to estimate the contribution of that parameter to the variance of the age. Where a parameter has an error that matches or exceeds the assigned value of the parameter (including the case of a parameter with an assigned value of zero, but with a non-zero error), a "one-sided" estimate of the error contribution is made.

## 6 Conclusion

The ROSY dating program provides a flexible tool for calculating ages and dose rates in situations involving planar geometry with up to three adjacent layers embedded in a sediment matrix. The user has considerable freedom to vary many parameters, including the compositions of all the media. In version 1.4, effects associated with dose gradients near boundaries for both alpha and beta radiation are modelled effectively, with these gradients extending to approximately 2mm for the beta dose and 40 micrometer for the alpha dose. ROSY provides more accurate estimates of dose rate, and thus in principle of age, than other software packages appropriate to planar geometry. The improvement mainly reflects the use of one-group theory in calculating beta doses.

As mentioned above, beta dose estimates can be made more accurate still with the proposed incorporation of data using dose-point-kernels based on Monte Carlo calculations. Another procedure being developed for ROSY will extend the range of uptake models to include coupled ESR and U-series data (Grün *et al.*, 1988). In principle, the sample age and uptake model parameters can be estimated simultaneously by fitting data on uranium series activity ratios as well as the equivalent dose (see for instance Schwarcz and Grün, 1993; Monigal *et al.*, 1997). This procedure can remove the restriction of age estimates to early and linear uptake (or combinations of early and linear uptake in different materials). We note that the ROSY calculations in this approach will provide a better beta dose estimate than was previously available. This ROSY approach is currently being applied to three sites in the Crimea, which form a significant set of U-series and ESR results where $^{14}C$ control is available (Rink *et al.*, 1998). Modification of ROSY to provide a more convenient user interface in a WINDOWS environment is also intended.

Prospective users of ROSY may obtain a copy of the latest version by contacting Lynn Falkiner at the McMaster University address of WJR and HPS, preferably by email to falkiner@mcmaster.ca.

## Acknowledgements

We thank J. Johnson for help with testing the latest versions of ROSY, and B. Blackwell for suggestions and testing. The reviewer provided helpful comments that have improved the presentation of the paper.

## References

Adamiec, G. and Aitken, M. (1998) Dose-rate conversion factors: update. *Ancient TL* **16,** 37-50.

Aitken, M. J. (1985) *Thermoluminescence Dating.* Academic Press, London.

Aitken, M. J. (1987) Alpha dose to a thin layer. *Ancient TL* **5,** 1-3.

Aitken, M. J., Clark, P. A. Gaffney, C. F. and Løvborg, L. (1985) Beta and gamma gradients. *Nuclear Tracks* **10,** 647-653.

Brennan, B. J., Rink, W. J., McGuirl, E. L., Schwarcz, H. P. and Prestwich, W.V. (1997) Beta doses in tooth enamel by "One-group" theory and the ROSY ESR dating software. *Radiation Measurements* **27,** 307-314.

De Canniere, P., DeBuyst, R., Dejehet, F., Apers, D. and Grün, R. (1986) ESR dating: a study of $^{210}Po$-coated geological and synthetic samples. *Nucl. Tracks Radiat. Meas.* **11,** 211-220.

Grün, R. (1986) Beta dose attenuation in thin layers. *Ancient TL* **4,** 1-8.

Grün, R. (1987) Alpha dose attenuation in thin layers. *Ancient TL* **5,** 6-8.

Grün, R. (1994) A cautionary note: use of 'water content' and 'depth for cosmic dose rate' in AGE and DATA programs. *Ancient TL* **12,** 50-51.

Grün, R. (1998) Comments on Brennan *et al.* Beta doses in tooth enamel by "One Group" theory and the ROSY ESR dating software. *Radiation Measurements* **29,** 579.

Grün, R., Schwarcz, H. P. and Chadam, J. (1988) ESR dating of tooth enamel: Coupled correction for U-uptake and U-series disequilibrium. *Nucl. Tracks Radiat. Meas.* **14,** 237-241.

Grün, R., Schwarcz, H. P. and Zymela, S. (1987) Electron spin resonance dating of tooth enamel. *Canadian Journal of Earth Science* **24,** 1022-1037.

Lyons, R. G. and Brennan, B. J. (1989) Alpha dose rate calculations in speleothem calcite: values of $\eta$ and $k_{eff}/k_{ref}$. *Ancient TL* **7,** 1-4.

Marsh, R. E. (1999) *Beta-Gradient Isochrons in Tooth Enamel using Electron Paramagnetic Resonance: Towards a New Dating Method in Archaeology.* McMaster University MSc thesis, in preparation.

Monigal, K., Marks, A. E., Demidenko, Yu. E., Rink, W. J., Schwarcz, H. P., Ferring, C. R. and McKinney, C. (1997) Nouvelles découvertes de restes humains au site Paléolithique Moyen de Starosele, Crimée (Ukraine). *Préhistore Européene* **11,** 11-31.

Nambi, K. S. V. and Aitken, M. J. (1986) Annual dose rate conversion factors for TL and ESR dating. *Archaeometry* **28,** 202-205.

O'Brien, K., Samson, S., Sanna, R. and McLaughlin, L. E. (1964) The application of "one-group" transport theory to beta-ray dosimetry. *Nuclear Science and Engineering* **18,** 90-96.

Prescott, J. R. and Hutton, J. T. (1994) Cosmic ray contributions to dose rates for luminescence and ESR dating: large depths and long-term time variations. *Radiation Measurements* **23,** 497-500.

Prestwich, W.V., Nunes, J.C. and Kwok, C.S.(1997) Beta interface dosimetry in the "one-group approximation". *Radiation Phys. Chem.* **49,** 509-513.

Rink, W.J. and Hunter, V.A. (1998) Densities of modern and fossil dental tissues: significance to ESR dating of tooth enamel. *Ancient TL* **15**, 20-27.

Rink, W. J., Lee, H. K., Rees-Jones, J. and Goodger, K. A. (1998) Electron spin resonance (ESR) and mass-spectrometric U-series dating of teeth in Crimean Middle Palaeolithic sites: Starosele, Kabazi II and Kabazi V. In *Palaeolithic of the Crimea Series*, Vol 1 (eds Marks, A. E. and Chabai, V. P.), pp 323-340. ERAUL, Liege.

Rink, W. J., Schwarcz, H. P., Stuart, A. J., Lister, A. M., Marseglia, E. and Brennan, B. J. (1996) ESR dating of the type Cromerian freshwater bed at West Runton, U.K. *Quaternary Science Reviews* **15,** 727-738.

Schwarcz, H. P. and Grün, R. (1993) Electron spin resonance (ESR) dating of the Lower Industry at Hoxne. In *The Lower Palaeolithic Site at Hoxne* (eds Gladfelter, B. G. and Wymer, J. J.), pp 210-211, Univ. Chicago Press, London.

Yang, Q., Rink, W. J. and Brennan, B. J. (1998) Experimental determinations of beta attenuation in planar dose geometry and application to ESR dating of tooth enamel. *Radiation Measurements* **29,** 663-671.

Ziegler, J. F., Biersack, J.P. and Littmark, U. (1985) *The stopping and range of ions in solids,* Vol 1 (ed Ziegler) Pergamon, New York.

**Reviewer**
R. Grün

**Comments**
It is unfortunate that the authors still use Fortran 77, which was a great at its release in 1977, but has outlived its use-by date by a great number of years. Reasonable graphic interfaces can be created by any more recent Fortran editor. The main reason for not using ROSY is the clumsiness of data inputs compared to a program such as DATA. However, this should not serve as an excuse to promote a scientifically outdated program (i.e. DATA).

# ESR analysis of fluorescence band in corals

Rainer Grün, Stuart Finley and Malcolm T. McCulloch

Research School of Earth Sciences
The Australian National University
Canberra ACT 0200, Australia

*(Received 26 November 1999; in final form 13 December 1999)*

Coral cores can provide a continuous record of the marine environment spanning over several hundred years. Using a variety of isotopic techniques it is possible to reconstruct palaeoclimates (e.g. Gagan *et al.* 1994, 1998; McCulloch *et al.* 1994, 1996, 1999) as well as environmental changes such as palaeofloods (Tudhope *et al.* 1995). One of the most interesting characteristics of coral sections from inshore regions is the occurrence of fluorescence bands. Some authors have attributed these to terrestrial fluvial discharge, where the corals incorporate humic substances during flood events. As a consequence, it was anticipated that sulfur-bearing components would generate the fluorescence (Isdale 1984). Others have argued that fluorescence bands are due to density changes resulting from stress from the low salinity flood plumes (Barnes and Taylor 1998).

Ikeda *et al.* (1992) measured an ESR scan on a 15 year slice of a coral from the Great Barrier reef. ESR measurements were carried out with a pin-hole cavity every 1 mm. The ESR spectra showed two main lines, those at g=2.0031 and g=2.0007 which have been attributed to $SO_3^-$ and $CO_2^-$, respectively (Debuyst *et al.* 1990, 1991, Barabas 1992, Barabas *et al.* 1992a,b). Ikeda *et al.* (1992) showed with doping experiments that the intensity of the ESR line at g=2.0031 increases with the amount of $SO_3^{2-}$ in aragonite, but was independent of $SO_4^{2-}$. Ikeda *et al.* (1992) also found a direct relationship between fluorescence bands and the intensity of g=2.0031 whilst intensity changes of g=2.0007 were attributed to differences in the density of the coral. In the ESR scan (Figure 2 of Ikeda *et al.* 1992), the signal at g=2.0007 showed more pronounced peaks than the signal at g=2.0031. Most of the peaks in the scan of the two signals were related, however, some larger peaks in the signal intensity of g=2.0007 were not reflected in the scan of g=2.0031.

In order to address the question whether fluorescence bands were attributable to increased sulfuric contents or density, we chose a coral core from Pandora Reef collected in late 1998. This section of the Great Barrier Reef is reached by the annual flood plumes discharged from the Burdekin River. A 1 cm thick slice was cut from the core which was exposed to UV light to identify the fluorescence bands (Figure 1). Rather than producing a continuous ESR scan, which would make it difficult to distinguish between fluorescence and density, samples were extracted for conventional ESR measurements. Four different fluorescence bands were chosen, three wide ones (1983 (A), 1974 (D) and 1968 (J)) and one rather thin one from the drought of 1969 (G). For comparison, additional samples were extracted from the non-fluorescent coral immediately above and below the fluorescence bands. Samples were drilled with a computerised high precision mill (Gagan *et al.* 1994, Alibert and McCulloch 1997). Sample weights varied between 27 and 51 mg.

For the measurement of the ESR signals at g=2.0031 and g=2.0007, the samples were irradiated with 5 kGy. Measurements were carried out at 2 and 100 mW. The signal at g=2.0057, which has been attributed to $SO_2^-$ (Barabas 1992), can be measured after thermal activation (Brumby and Yoshida 1994, Martinez Walter 1994,Yoshida and Brumby 1999). Prior to the measurement of g=2.0057, the samples were heated for 7h at 150 °C. The ESR spectra are shown in Figure 2. However, as can be seen in Figure 2A, the irradiated, non-heated corals also show a small signal at g=2.0057.

Figure 3 shows the intensity measurements of all signals in all samples (normalised on weight). If fluorescence was related to $SO_2^-$ (g=2.0057) or $SO_3^-$ (g=2.0031), the respective signal intensities of samples A, D, G and J would be higher than either of the two surrounding ones. Figure 3 and Table 1 show clearly that this is not the case. The signal at g=2.0057 shows some relationship with the fluorescence bands before heating. However, the very small signal intensities

made quantitative analysis very uncertain and the variations seem within the statistical uncertainty of the ESR measurement. Note that just by chance, signals of approximately the same intensity would yield one to two «Y's» in Table 1.

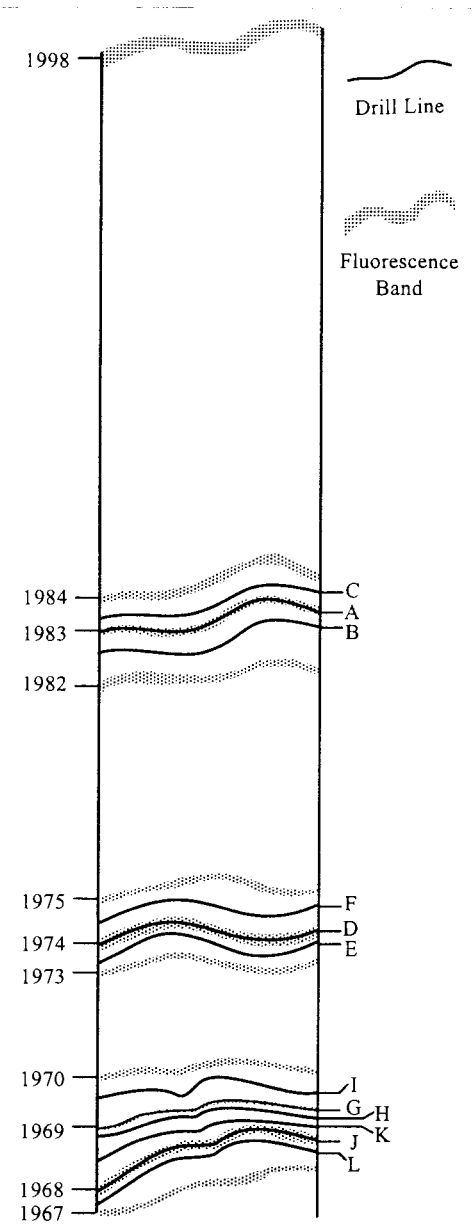


***Figure 1.***
*Coral section from the Pandora Reef spanning 32 years between 1967 and 1998.*

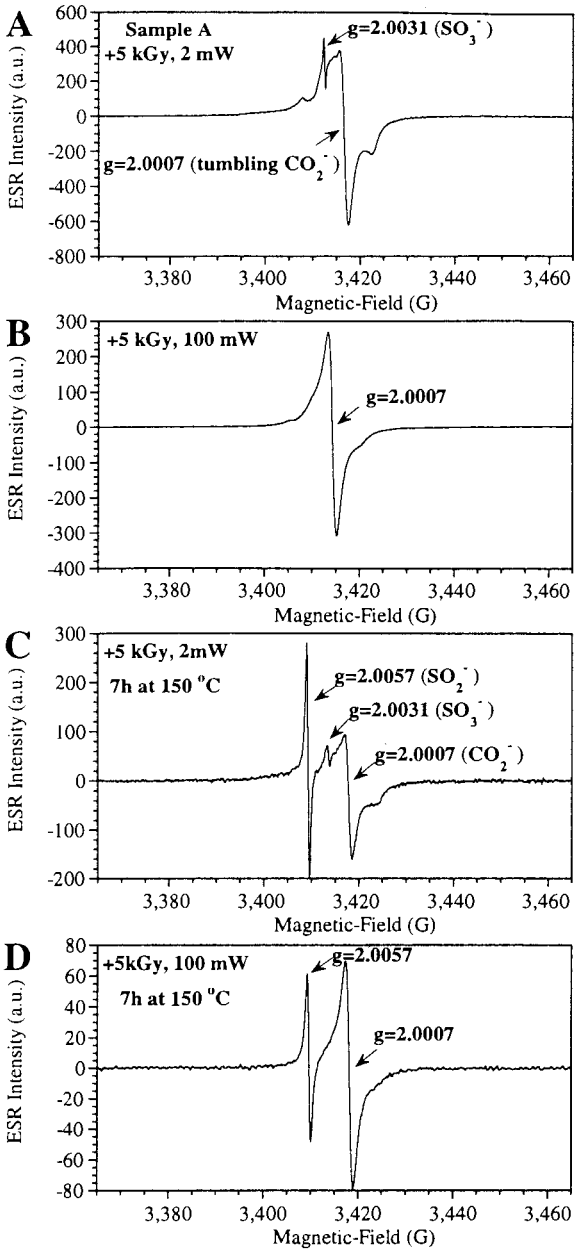


***Figure 2.***
*ESR spectra*

For three out of four sets, the intensity of g=2.0007 is related to the fluorescence band. These peaks are also by far the most pronounced ones, similar to the finding of Ikeda *et al.* (1992). Because it is thought that the signal at g=2.0007 is a surface defect (Barabas *et al.* 1992a) and linked to crystal water molecules (Debuyst *et al.* 1991), the peaks of the samples D, G and J may

indicate that fluorescence bands are related to the incorporation of water molecules into the crystal lattice or increased internal surface area. The latter hypothesis is consistent with the inferences of Barnes and Taylor (1998) that density and related surface area changes are the main cause of fluorescence.

Figure 2 shows that the signal at g=2.0057 shows severe microwave power saturation effects (compare 2C and 2D). Thus, it is advisable to measure this signal at low microwave powers for quantitative analyses.

We attribute the differences between our results and those of Ikeda *et al.* (1992) to the fact that intensity measurements using a pin hole cavity are critically dependent of the density of the sample. Rather than being an indicator of variation in the concentration of $SO_3^-$, the intensity of the signal at g=2.0031 recorded the density of the coral slice. The signal at g=2.0007 seems to be related to the fluorescence bands, but the crystallographic aspect has to await further investigation. We conclude that the fluorescence bands of the coral investigated are neither related to $SO_3^-$ (and by implication to $SO_3^{2-}$) nor to $SO_2^-$.

| | 5 kGy | | | | 5 kGy, 7 h at 150 °C | | | | |
|---|---|---|---|---|---|---|---|---|---|
| Sample Set | 2.0057 | 2.0031 | 2.0007 | **2.0007** | 2.0057 | 2.0031 | 2.0007 | **2.0057** | **2.0007** |
| CAB | Y | N | N | N | N | N | N | N | N |
| FDE | N | N | Y | Y | N | N | Y | N | Y |
| IGH | Y | N | Y | Y | N | N | N | N | Y |
| KJL | Y | N | Y | Y | N | N | Y | N | Y |

**Table 1:** Summary of ESR measurements (bold: measurement at 100 mW. Y: ESR signal of fluorescent sample is higher than either of the two surrounding samples; N: it is not higher)

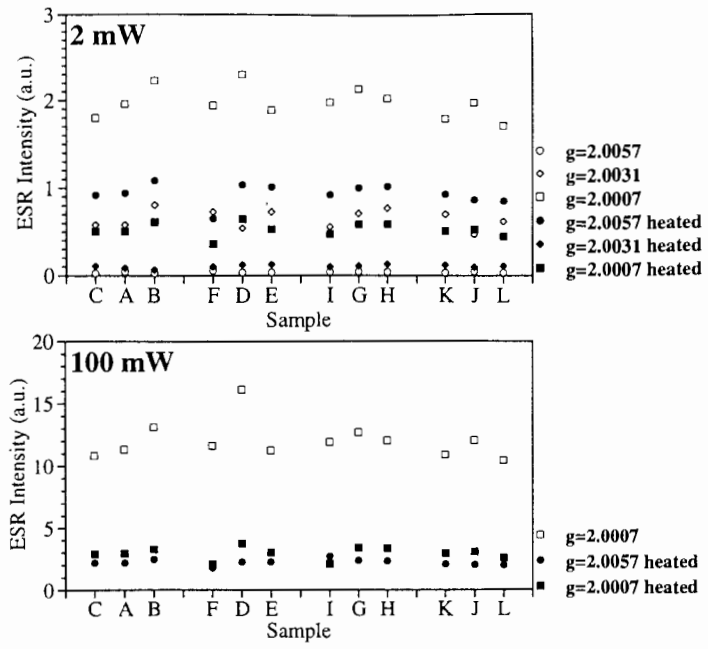


***Figure 3.***
*Intensity measurements of the sample sets shown in Figure 1.Only the signal at g=2.0007 shows a relationship between intensity and fluorescence*

**References**

Alibert, C. and McCulloch, M.T. (1997) Strontium/calcium rtios in modern Porites corals from the Great Barrier Reef as a proxy for sea surface temperature: Calibratoin of the thermometer and monitoring of ENSO. *Paleoceanography* **12**: 345-363.

Barabas, M. (1992) The nature of the paramagnetic centres at $g$ = 2.0057 and $g$ = 2.0031 in marine carbonates. *Nuclear Tracks and Radiation Measurements* **20**: 453-464.

Barabas, M., Mudelsee, M., Bach, A., Walther, R. and Mangini, A. (1992a) General properties of the paramagnetic centre at g=2.0006 in carbonates. *Quaternary Science Reviews* **11**: 165-171.

Barabas, M., Mudelsee, M., Walther, R. and Mangini, A. (1992b) Dose response and thermal behavior of the ESR signal at g=2.0006 in carbonates. *Quaternary Science Reviews* **11**: 173-179.

Barnes, D.J. and Taylor, R.B. (1998) On the nature of Luminescence in coral skeletons. *CRC Reef Research Technical Report* **22:** 1-38 .

Brumby, S. and Yoshida, H. (1994) ESR dating of mollusk shell: Investigations with modern shell of four species. *Quaternary Science Reviews* **13**: 157-162.

Debuyst, R., Bidiamambu, M. and Dejehet, F. (1990) Diverse $CO_2^-$ radicals in g-and a-irradiated synthetic calcite. *Bull. Soc. Chim. Belg.* **99**: 535-541.

Debuyst, R., Bidiamambu, M. and Dejehet, F. (1991). An EPR study of g- and a-irradiated synthetic powdered calcite labelled with carbon 13. *Nuclear Tracks and Radiation Measurements* **18**: 193-201.

Gagan, M. K., Ayliffe, L.K., Hopley, D., Cali, J.A., Mortimer, G. E., Chappell, J., McCulloch, M.T. and Head, M.J. (1998) Temperature and surface-ocean water balance of the mid-Holocene tropical western Pacific. *Science* **279**: 1014-1018.

Gagan, M.K., Chivas, A.R. and Isdale, P.J. (1994) High-resolution isotopic records from corals using ocean temeprature and mass spawning chronometers. *Earth and Planetary Science Letters* **121**: 549-558.

Ikeda, S., Neil, D., Ikeya, M., Kai, A. and Miki, T. (1992) Spatial variation of $CO_2^-$ and $SO_3^-$ radicals in massive coral as environmental indicator. *Japanese Journal of Applied Physics* **31**: 1644-1646.

Isdale P. (1984) Fluorescent bands in massive corals record centuries of coastal rainfall. *Nature* **310**: 578-579.

McCulloch, M.T., Gagan, M.K., Mortimer, G.E., Chivas, A.R. & Isdale, P.J. (1994) A high resolution Sr/Ca and d18O coral record from the Great Barrier Reef, Australia, and the 1982-83 El Niño. *Geochim. Cosmochim. Acta* **58**: 2747-2754.

McCulloch, M.T., Mortimer, G.E., Esat, T., Xianhua, Li., Pillans, B. and Chappell, J. (1996) High resolution windows into early-Holocene climate: Sr/Ca coral records from the Huon Peninsula. *Earth Planet. Sci. Lett.* **138**: 169-178.

McCulloch, M.T., Tudhope, A.W., Esat, T. M., Mortimer, Chappell, J . Pillans, B., Chivas A.R., and Omura A. 1999. Coral record of equatorial sea-surface temperatures during the penultimate deglaciation at Huon Peninsula. *Science* **283**: 202-204.

Martinez Walter, M. (1994) ESR Datierung an Karbonaten mit dem $SO_2^-$ Radikal. Unpublished Diplom Arbeit, Fakultät für Physik und Astronomie, Ruprechts-Karls-Universität Heidelberg,106 p..

Yoshida, H. and Brumby, S. (1999) Comparison of ESR ages of corals using different signals at X- and Q-band: Re-examinations of corals from Huon Peninsula, Papua New Guinea. Quaternary Science Reviews (in press).

**Reviewer**

H. Schwarcz

**Comments**

The authors have attempted to confirm an earlier study suggesting that fluorescent bands in coral are due to sulfur oxy-anion radicals. Although they observe some weak enhancements in the intensity of some of these signals, they do only see weak enhancements of these signals in the fluorescent bands. However, one of the strongest signal enhancements is seen in the g = 2.0007 peak associated with $CO_2^-$, which could be strengthened as a result of difference in the texture of the coral (i.e., the packing density or mean size of aragonite crystals in the coral skeleton). This lends support to the idea of that fluorescence occurs preferentially in bands of higher density. It would be desirable to complement any further ESR studies of this problem with complementary, quantitative studies of the fluorescence phenomenon itself, as it is not clear in the present studies whether the material adjacent to fluorescent bands is totally non-fluorescent or is simply less so. As well, more detailed, quantification of coral density would be useful.

# Sampling in waterlogged sands with a simple hand-operated corer

Jakob Wallinga[1] and Jan van der Staay[2]

1. Netherlands Centre for Geo-ecological Research, Faculty of Geographical Sciences, Utrecht University, P.O. Box 80115, NL-3508 TC Utrecht, The Netherland
J.Wallinga@geog.uu.nl
2. Pastoor Savenijelaan 16, NL-6678 BK Oosterhout, The Netherlands.

*(Received 7 Dec. 1999)*

## Introduction

Sampling for luminescence dating requires the collection of uncontaminated sediments that have not been exposed to light during sampling. Exposures enable very easy sampling, but unfortunately they are sparse in most environments. In lowland areas the groundwater table is often relatively close to the surface, which makes man-made exposures fill with water rapidly. Drainage is extremely costly, and therefore normally not feasible for scientific purposes. In the absence of exposures, samples have to be taken using some sort of coring device. However, most suitable devices available are mechanical and consequently heavy, which makes drilling problematic both because of the costs involved and the logistic requirements. Hand-operated coring devices offer major advantages over mechanical drilling in both aspects. In this paper we describe the Van der Staay suction corer, which is a simple hand-operated coring device. The corer is suitable for taking samples from waterlogged sands to a depth of some 10 meters without contamination or light exposure.

## The corer

The Van der Staay suction-corer was developed at the Geological Survey of the Netherlands in the early 1970's. Van de Meene *et al.* (1979) provided a detailed description of the equipment and its use. That publication is however difficult to obtain, therefore we will briefly discuss the construction and working of the Van der Staay suction-corer. People interested in the original publication should feel free to contact us in order to receive a copy of that paper. The basic parts of the corer are outlined in figure 1. The corer consists of two PVC tubes, of which the outer tube normally has a diameter of 35mm. The outer tube works both as casing as well as a corer. The inner tube fits into the outer tube and is fitted with a leather cup on its lower end. The leather cup allows the user to suck a vacuum facilitating the penetration of the outer tube into the sand (fig. 1). The corer only works in waterlogged sandy deposits, since otherwise no vacuum can be created. After coring, both tubes are extracted from the hole together, and in standard use the sampled material is squeezed out of the tube to allow examination.

Prior to using the Van der Staay suction-corer, a hole has to be drilled penetrating the non-saturated layer at the surface using a simple hand auger (fig. 1A). Van der Staay suction-corers of different lengths (2.5 and 5 metres) are used for coring to different depths in water saturated sand. Extension tubes of two and a halve metres or five metres in length enable routine coring to depths of some ten metres. However, even depths up to 30 metres have been reached according to Van de Meene *et al.* (1979). An extension tube is tightly fitted into a widened bottom end of the main corer and can be connected and disconnected manually. For holes penetrating more than 3 meters of waterlogged sand, the hole is normally drilled in several steps of a few metres each using the corers of different lengths and if necessary an extension tube. After every step the entire corer is extracted from the hole, which results in collapse of the hole. Experience has however learned that the tubes can be quite easily pushed back to the depth reached during the prior step. Ideally the corer is pushed back to this depth while the inner tube is attached to the outer tube, so that no material from this course is sampled. The corer is relatively easy and cheap to construct, and also easy to transport and operate. Two to three people are needed to handle the corer. The corer has been widely used in The

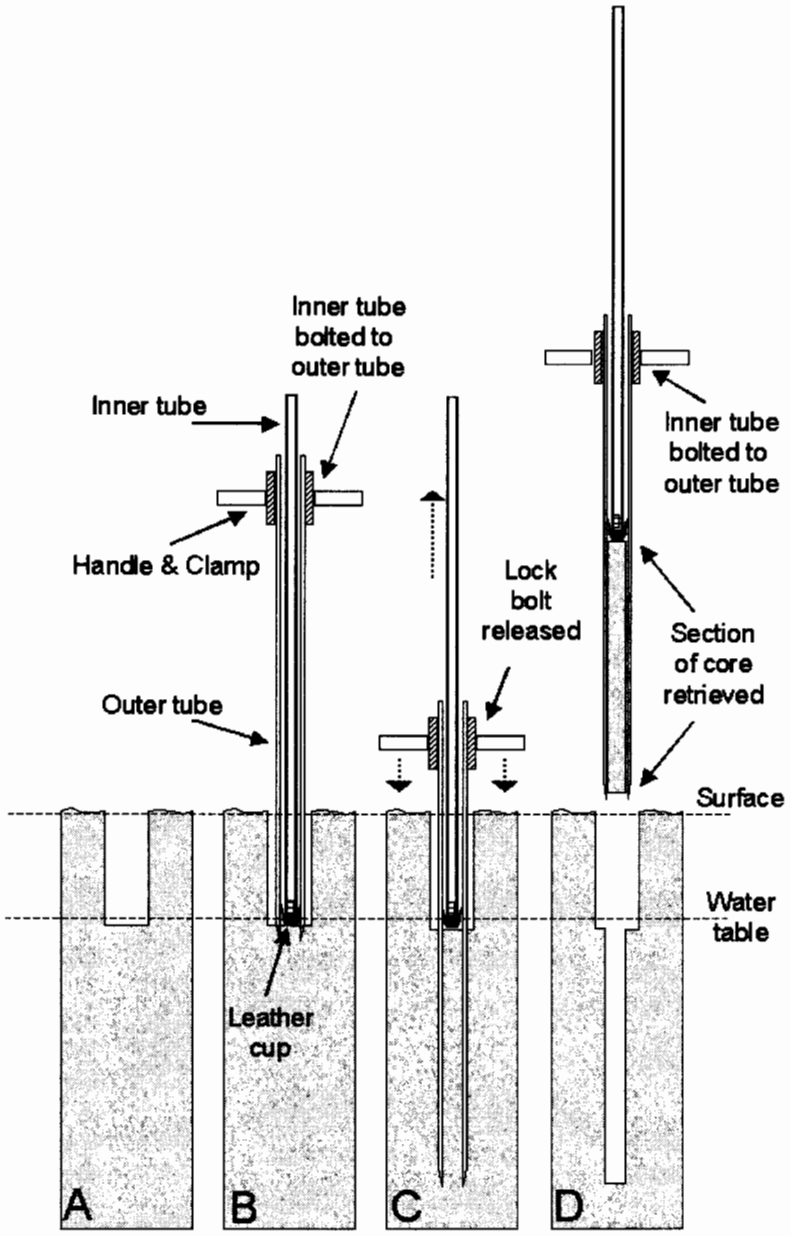


***Figure 1.*** *Basic parts of the Van der Staay suction-corer, as well as the working principles (adapted from van de Meene et al., 1979).*
*A – Hole penetrating to water saturated zone, drilled with auger.*
*B – Van der Staay suction-corer is placed into the hole.*
*C – The outer tube is pushed down while inner tube is kept in place, or pulled slightly upwards to create a vacuum.*
*D – The inner tube is bolted to the outer tube, subsequently the corer, including core, is extracted from the hole.*

Netherlands (e.g. Törnqvist *et al.*, 1993) and also in Asia.

## Sampling

Samples for luminescence dating have to be retrieved without light exposure to prevent bleaching of the luminescence signal. To enable us to do so we had to modify the Van der Staay suction-corer slightly. The lower end of the outer tube was fitted with a sampling tube of the same diameter and about 30cm in length. The length of the sampling tube can be varied depending on the amount of sample needed for analysis. The sampling tube is fitted into a widened lower end of the corer, in the same way as the extension tube is.

To obtain a sample, a hole is drilled to the water table using an auger. Then the suction-corer is placed in the hole and the lock-bolt fixing the inner tube to the outer tube released. Subsequently the outer tube is pushed to the lower depth of the sample, while the inner tube of the corer is alternately pulled and released in order to create a vacuum, which facilitates the penetration of the outer core. When the lower sampling depth is reached the inner tube is fixed to the outer tube by the use of the lock bolt on the top of the outer tube. The corer is then carefully extracted from the hole to ensure that no sample falls out of the tube. The system relies on the suction created in the tube to prevent the sample from falling out. As soon as the lower end of the corer reaches the surface, a black plastic cap is used to seal the lower end of the sample tube. It is advisable to pinch a small hole in the cap to allow water to drain. After sealing the lower end, the corer is laid flat on the ground and the inner tube is squeezed into the outer tube to drain excessive water and push the sample firmly into the sample tube. Subsequently the corer is put upright again; the sampling tube is disconnected from the main corer and immediately sealed with a black plastic cap. At this point it is ensured that the sample tube is completely full so that the light exposed outer ends are fixed. The outer ends are discarded off in a lab under subdued red light conditions. The remaining sample has never been exposed to any light and is therefore suitable for luminescence dating.

## Experience and conclusion

We have used the modified Van der Staay suction-corer to obtain samples from fluvial channel deposits in the Rhine-Meuse delta (The Netherlands). All samples were sandy and saturated with water. The Van der Staay suction-corer proved to be a very useful piece of equipment in obtaining samples to a depth of 7 meters. Several samples can be taken from the same hole at different depths by coring in several steps. We were able to take up to 12 samples in a field day, operating the corer with three people. The OSL dating results did not show any indication of light exposure during sampling (Wallinga and Duller, in press). We conclude that the Van der Staay suction-corer is a suitable corer to obtain samples for luminescence dating from relatively shallow, water saturated sands. The corer is cheap and easy to construct, operate and transport which provides big advantages over other coring techniques used to obtain samples for luminescence dating.

## References

Van de Meene, E.A., Van der Staay, J. and Teoh Lay Hock (1979) The Van der Staay Suction-corer – a Simple Apparatus for Drilling in Sand below Groundwater Table. Rijks Geologische Dienst, Haarlem.

Törnqvist, T.E., Van Ree, M.H.M. and Faessen, E.L.J.H. (1993) Longitudinal facies architectural changes of a Middle Holocene anastomosing distributary system (Rhine-Meuse delta, central Netherlands). *Sedimentary Geology*, 85, 203-219.

Wallinga, J. and Duller, G.A.T. in press. The effect of optical absorption on the infra-red stimulated luminescence age obtained on coarse-grain feldspar. *Quaternary Science Reviews (Quaternary Geochronology)*.

## Reviewer

Geoff Duller

# Obituary

## Prof. Huang Peihua

Peihua Huang, Professor of Geography at the University of Science and Technology of China, died at the age of 67 in an accident on 27th February 1999.

Prof. Huang was born on October 1931 and graduated at the Geographic Department of Nanjing University in 1952 and in 1959 as a postgraduate student. He specialized in teaching and research work on the Quaternary Environment and Chronology, seismo-geology and geodynamics. He queried the validity of Professor Li Siguang's book "The Ice-Age of Lushan Mountain". In the 1960's he developed a number of thorough research projects on the characteristics of the evolution of the Quaternary Environment of China. In the beginning of 1980's he developed a program to study mantle convection and the stress patterns under the lithosphere. He was the first to introduce the new dating technique of electron spin resonance (ESR) in China. He and his research group established and developed ESR research and in 1989 he determined the burial age of the first skull of Peking Man. This attracted scientific attention worldwide.

Professor Peihua Huang's research work was internationally acknowledged. He developed collaboration with scholars in Japan, America, Canada, Germany, Australia, France etc. He traveled repeatedly to these countries and received many international colleagues for research exchange in Hefei. He attended many international conferences and exchanged his ideas with the leading scholars. Professor Huang made decisive contributions to our understanding of the Quaternary Environment and Chronology.

Professor Huang was a strict, sincere and generous man. His death causes grief among colleagues, students, relatives and friends at home and abroad. His death is a great loss to the field of geology science and he will be thoroughly missed.

Liang Renyou
Chen Tiemei

*Ancient TL* vol 17 No.2 1999

# Thesis Abstract

**Thesis title :** Electron paramagnetic resonance dosimetry : methodology and material characterization
**Author :** Robert Hayes
**Date :** August 4, 1999
**Supervisor :** Edwin H. Haskell
**University :** University of Utah

Electron Paramagnetic Resonance (EPR) methodologies for radiation dose reconstruction are investigated using various dosimeter materials. Specifically, methodologies were developed and used that were intended to improve the accuracy and precision of EPR dosimetric techniques, including combining specimen rotation during measurement, use of an internal manganese standard, instrument stabilization techniques and strict measurement protocols. Characterization and quantification of these improvements were preformed on three specific EPR dosimeter materials. The dosimeter materials investigated using these optimized EPR techniques were Walrus teeth, human tooth enamel and alanine dosimeters. Walrus teeth showed the least desirable properties for EPR dosimetry yielding large native signals and low sensitivity (EPR signal per unit dose). The method for tooth enamel and alanine resulted in large improvements in precision and accuracy. The minimum detectable dose (MDD) found for alanine was approximately 30 mGy (three standard deviations from the measured zero dose value). This is a sensitivity improvement of 5 to 10 over other specialized techniques published in the literature that offer MDD's in the range of 150 mGy to 300 mGy. The accuracy of the method on tooth enamel was comparable to that typically reported in the literature although the measurement precision was increased by about 7. This improvement in measurement precision enables various applications including dose vs. depth profile analysis and a more non destructive testing evaluation (where the whole sample need not be additively irradiated in order to calibrate its radiation response). A non destructive evaluation of numerous samples showed that the method could reconstruct the same doses to within 10 mGy of those evaluated destructively. Doses used for this assessment were in the range of 100 to 250 mGy. The method had sufficient stability to measure tooth enamel samples exhibiting extreme anisotropy with a precision of approximately 5%. This is a significant improvement since the dosimetric EPR signal from a single tooth enamel grain may vary by as much as 50% depending on its orientation in the cavity.

*For copies of this dissertation, contact UMI Dissertation Services, 300 North Zeeb Road, PO Box 1346, Ann Arbor, MI 48106-1346; Tel : (734) 761-4700; http://www.umi.com/*

# Bibliography

(From 1 April 1999 to 30 October 1999) Compiled by **Ann Wintle**


Akselrod A., Akselrod M. S., Agersnap Larsen N., Banerjee D., Bøtter-Jensen L., Christensen P., Lucas A. C., McKeever S. W. S., and Yoder C. (1999) Optically stimulated luminescence response of $Al_2O_3$:C to beta radiation. *Radiation Protection Dosimetry* **85**, 125-128.

Akselrod M. S., Agersnap Larsen N., Whitley V., and McKeever S. W. S. (1998) Thermal quenching of F-center luminescence in $Al_2O_3$:C. *Journal of Applied Physics* **84**, 3364-3373.

Akselrod M. S., Agersnap Larsen N., Whitley V., and McKeever S. W. S. (1999) Thermal quenching of F centre luminescence in $Al_2O_3$:C. *Radiation Protection Dosimetry* **84**, 39-42.

Akselrod M. S. and McKeever S. W. S. (1999) A radiation dosimetry method using pulsed optically stimulated luminescence. *Radiation Protection Dosimetry* **81**, 167-176.

Alvarez S., Calderon T., Millan A., Beneitez P., Piters T. M., Barboza M., Jaque F., and Garcia Sole J. (1999) Photoluminescence decay of irradiated herbs. *Radiation Protection Dosimetry* **85**, 477-480.

Amit R., Zilberman E., Porat N., and Enzel Y. (1999) Relief inversion in the Avrona Playa as evidence of large-magnitude historical earthquakes, southern Arava Valley, Dead Sea Rift. *Quaternary Research* **52**, 76-91.

Baietto V., Villeneuve G., Schvoerer M., Bechtel F., and Herz N. (1999) Investigation of electron paramagnetic resonance peaks in some powdered Greek white marbles. *Archaeometry* **41**, 253-265.

Bailiff I. K. (1999) The development of retrospective luminescence dosimetry for dose reconstruction in areas downwind of Chernobyl. *Radiation Protection Dosimetry* **84**, 411-420.

Bailiff I. K. and Clark R. J. (1999) A preliminary study of fast time-resolved luminescence in $Al_2O_3$:C. *Radiation Protection Dosimetry* **84**, 457-460.

Bailiff I. K. and Petrov S. (1999) The use of the 210°C TL peak in quartz for retrospective dosimetry. *Radiation Protection Dosimetry* **84**, 551-554.

Banerjee D., Bøtter-Jensen L., and Murray A. S. (1999) Retrospective dosimetry: preliminary use of the single aliquot regeneration (SAR) protocol for the measurement of quartz dose in house bricks. *Radiation Protection Dosimetry* **84**, 421-426.

Banerjee D., Singhvi A. K., Pande K., Gogte V. D., and Chandra B. P. (1999) Towards a direct dating of fault gouges using luminescence dating techniques - methodological aspects. *Current Science* **77**, 256-268.

Bateman M. D. (1998) The origin and age of coversand in N. Lincolnshire, U.K. *Permafrost and Periglacial Processes* **9**, 313-325.

Bateman M. D. and Holmes P. J. (1999) Orange River alluvial terraces: is luminescence dating a useful tool? *South African Journal of Science* **95**, 57-58.

Bateman M. D. and Van Huissteden J. (1999) The timing of last glacial periglacial and aeolian events, Twente, eastern Netherlands. *Journal of Quaternary Science* **14**, 277-283.

Bateman M. R. and Diez Herrero A. (1999) Thermoluminescence dates and palaeoenvironmental information of the late Quaternary sand deposits, Tierra de Pinares, Central Spain. *Catena* **34**, 277-291.

Bøtter-Jensen L., Banerjee D., Jungner H., and Murray A. S. (1999) Retrospective assessment of environmental dose rates using optically stimulated luminescence with $Al_2O_3$:C and quartz. *Radiation Protection Dosimetry* **84**, 537-542.

Bøtter-Jensen L., Duller G. A. T., Murray A. S., and Banerjee D. (1999) Blue light emitting diodes for optical stimulation of quartz in retrospective dosimetry and dating. *Radiation Protection Dosimetry* **84**, 335-340.

Bøtter-Jensen L. and Murray A. S. (1999) Developments in optically stimulated luminescence techniques for dating and retrospective dosimetry. *Radiation Protection Dosimetry* **84**, 307-316.

Bourman R. P., Belperio A. P., Murray Wallace C. V., and Cann J. H. (1999) A last interglacial embayment fill at Normanville South Australia, and its neotectonic implications. *Transactions of the Royal Society of South Australia* **123**, 1-15.

Bulur E. and Göksu H. Y. (1999) Phototransferred thermoluminescence from $Al_2O_3$:C using blue light emitting diodes. *Radiation Measurements* **30**, 203-206.

Chen R. and Leung P. L. (1999) Modelling the pre-dose effect in thermoluminescence. *Radiation Protection Dosimetry* **84**, 43-46.

Clarke M. L., Rendell H. M., and Wintle A. G. (1999) Quality assurance in luminescence dating. *Geomorphology* **29**, 173-185.

Colyott L., McKeever S. W. S., and Akselrod M. S. (1999) An integrating UVB dosemeter system. *Radiation Protection Dosimetry* **85**, 309-312.

Correcher V., Garcia-Guinea J., Delgado A., and Sanchez-Munoz L. (1999) Spectra thermoluminescence emissions and continuous trap distribution of a cross-hatch twinned low microcline. *Radiation Protection Dosimetry* **84**, 503-506.

Correcher V., Gomez-Ros J. M., and Delgado A. (1999) The use of albite as a dosemeter in accident dose reconstruction. *Radiation Protection Dosimetry* **84**, 547-550.

DeNava J. M. M., Gorsline D. S., Goodfriend G. A., Vlasov V. K., and CruzOrozco R. (1999) Evidence of Holocene climatic changes from aeolian deposits in Baja California Sur, Mexico. *Quaternary International* **56**, 141-154.

Duller G. A. T., Bøtter-Jensen L., Murray A. S., and Truscott A. J. (1999) Single grain laser luminescence (SGLL) measurements using a novel automated reader. *Nuclear Instruments and Methods in Physics Research B* **155**, 506-514.

Duller G. A. T., Bøtter-Jensen L., Kohsiek P., and Murray A. S. (1999) A high-sensitivity optically stimulated luminescence scanning system for measurement of single sand-sized grains. *Radiation Protection Dosimetry* **84**, 325-330.

Eriksson M. G., Olley J. M., and Payton R. W. (1999) Late Pleistocene colluvial deposits in central Tanzania; erosional response to climatic change? *GFF* **121**, 198-201.

Fang X.-M., Ono Y., Fukusawa H., Pan B.-T., Li J.-J., Guan D.-H., Oi K., Tsukamoto S., Torii M., and Mishima T. (1999) Asian summer monsoon instability during the past 60,000 years: magnetic susceptibility and

pedogenic evidence from the western Chinese Loess Plateau. *Earth and Planetary Science Letters* **168**, 219-232.

Folz E. and Mercier N. (1999) Use of a new procedure to determine paleodose in the OSL dating of quartz: the MARA protocol. *Quaternary Science Reviews* **18**, 859-864.

Forman S. L. (1999) Infrared and red stimulated luminescence dating of Late Quaternary near-shore sediments from Spitsbergen, Svalbard. *Arctic, Antarctic, and Alpine Research* **31**, 34-49.

Frechen M. (1999) Luminescence dating of loessic sediments from the Loess Plateau , China. *Geologische Rundschau* **87**, 675-684.

Frechen M. and Yamskikh A. F. (1999) Upper Pleistocene loess stratigraphy in the southern Yenisei Siberia area. *Journal of the Geological Society* **156**, 515-525.

Galbraith R. F., Roberts R. G., Laslett G. M., Yoshida H., and Olley J. M. (1999) Optical dating of single and multiple grains of quartz from Jinmium rock shelter (northern Australia); Part I, Experimental design and statistical models. *Archaeometry* **41**, 339-364.

Garcia-Guinea J., Correcher V., and Delgado A. (1999) The potential use of annealed high-albite ($AlSi_3O_8Na$) as an ultraviolet radiation dosimeter. *Journal of Material Science Letters* **18**, 1263-1265.

Garcia-Guinea J., Correcher V., and Valle-Fuentes F. (1999) Thermoluminescence of kaolinite. *Radiation Protection Dosimetry* **84**, 507-510.

Gilbertson D. D., Schwenninger J.-L., Kemp R. A., and Rhodes E. J. (1999) Sand-drift and soil formation along an exposed North Atlantic coastline:14,400 years of diverse geomorphological, climatic and human impacts. *Journal of Archaeological Science* **26**, 439-469.

Gonzalez P., Azorin J., Schaaf P., and Ramirez A. (1999) Assessing the potential of thermoluminescence dating of pre-conquest ceramics from Calixtlahuaca, Mexico. *Radiation Protection Dosimetry* **84**, 483-488.

Gotze J., Habermann D., Kempe U., Neuser R. D., and Richter D. K. (1999) Cathodoluminescence microscopy and spectroscopy of plagioclases from lunar soil. *American Mineralogist* **84**, 1027-1032.

Gotze J., Plotze M., Fuchs H., and Habermann D. (1999) Defect structure and luminescence behaviour of agate - results of electron paramagnetic (EPR) and cathodoluminescence (CL) studies. *Mineralogical Magazine* **63**, 149-167.

Han Z. Y., Li S.-H., and Tso M. Y. W. (1999) TL dating technique based on the trap model and its application as a geochronometer for granitic quartz. *Radiation Protection Dosimetry* **84**, 471-478.

Hutt G., Jaek I., Brodski L., and Vasilchenko V. (1999) Optically stimulated luminescence characteristics of natural and doped quartz and alkali feldspars. *Applied Radiation and Isotopes* **50**, 969-974.

Jaek I., Hutt G., and Streltsov A. (1999) Study of deep traps in alkali feldspars and quartz by the optically stimulated afterglow. *Radiation Protection Dosimetry* **84**, 467-470.

Keen D. H., Bateman M. D., Coope G. R., Field M. H., Langford H. E., Merry J. S., and Mighall T. M. (1999) Sedimentology, palaeoecology and geochronology of Last Interglacial deposits from Deeping St James, Lincolnshire, England. *Journal of Quaternary Science* **14**, 411-436.

Lamothe M. and Auclair M. (1999) A solution to anomalous fading and age shortfalls in optical dating of feldspar minerals. *Earth and Planetary Science Letters* **171**, 319-323.

Lang A., Kadereit A., Behrends R.-H., and Wagner G. A. (1999) Optical dating of anthropogenic sediments at the archaeological site of Herrenbrunnenbuckel, Bretten-Auerbach (Germany). *Archaeometry* **41**, 397-411.

Li S.-H., Tso M.-Y., Westaway K. E., and Chen G. (1999) Choice of the most appropriate thermal treatment in optical dating of quartz. *Radiation Protection Dosimetry* **84**, 495-498.

Lucas A. C. and Lucas B. K. (1999) High dose TL response of $Al_2O_3$:C single crystals. *Radiation Protection Dosimetry* **85**, 455-458.

Mahat R. H., Amin Y. M., Jaafar Y. M., Prakash R., and Vengadaesvaran B. (1998) Thermoluminescence dating of Gua Tok Long prehistoric site in Malaysia. *Radiation Physics and Chemistry* **51**, 713.

Mauz B. (1999) Late Pleistocene records of littoral processes at the Tyrrhenian Coast (Central Italy); depositional environments and luminescence chronology. *Quaternary Science Reviews* **18**, 1173-1184.

McKeever S. W. S. and Akselrod M. S. (1999) Radiation dosimetry using pulsed optically stimulated luminescence of $Al_2O_3$:C. *Radiation Protection Dosimetry* **84**, 317-320.

Michael C. T., Zacharias N., Polikreti K., and Pagonis V. (1999) Minimising the spurious TL of recently fired ceramics using the foil technique. *Radiation Protection Dosimetry* **84**, 499-502.

Murray A. S. and Olley J. M. (1999) Determining sedimentation rates using luminescence dating. *GeoResearch Forum* **5**, 121-144.

Murray A. S. and Wintle A. G. (1999) Sensitisation and stability of quartz OSL: implications for interpretations of dose response curves. *Radiation Protection Dosimetry* **84**, 427-432.

Murray-Wallace C. V., Belperio A. P., Bourman R. P., Cann J. H., and Price D. M. (1999) Facies architecture of a last interglacial barrier: a model for Quaternary barrier development from the Coorong to Mount Gambier Coastal Plain, southeastern Australia. *Marine Geology* **158**, 177-195.

Nagatomo T., Kajiwara H., Fujimura S., Kamada T., and Yokoyama Y. (1999) Luminescence dating of tephra from paleolithic sites in Japan (from 10 ka to 500 ka). *Radiation Protection Dosimetry* **84**, 489-494.

O'Connor P. W. and Thomas D. S. G. (1999) The timing and environmental significance of Late Quaternary linear dune development in western Zambia. *Quaternary Research* **52**, 44-55.

Oczkowski H. L. and Przegietka K. R. (1998) Partial matrix doses for thermoluminescence dating. *Physica Scripta* **58**, 534-537.

Olley J. M., Caitcheon G. G., and Roberts R. G. (1999) The origin of dose distributions in fluvial sediments, and the prospect of dating single grains from fluvial deposits using optically stimulated luminescence. *Radiation Measurements* **30**, 201-217.

Owen L. A., Cunningham D., Richards B. W. M., Rhodes E., Windley B. F., Dorjnamjaa D., and Badamgarav J. (1999) Timing of formation of forebergs in the northeastern Gobi Altai, Mongolia: implications for estimating mountain uplift rates and earthquake recurrence intervals. *Journal of the Geological Society* **156**, 457-464.

Pinnioja S., SiitariKauppi M., Jernstrom J., and Lindberg A. (1999) Detection of irradiated foods by luminescence of contaminating minerals - effect of mineral composition on luminescence intensity. *Radiation Physics and Chemistry* **55**, 743-747.

Pinnioja S., SiitariKauppi M., and Lindberg A. (1999) Effect of feldspar composition on thermoluminescence in minerals separated from food. *Radiation Physics and Chemistry* **54**, 505-516.

Porat N., Zhou L. P., Chazan M., Noy T., and Horwitz L. K. (1999) Dating the Lower Paleolithic open-air site of Holon, Israel by luminescence and ESR techniques. *Quaternary Research* **51**, 328-341.

Price D. M., Bryant E. A., and Young R. W. (1999) Thermoluminescence evidence for the deposition of coastal sediments by tsunami wave action. *Quaternary International* **56**, 123-128.

Roberts R. G., Galbraith R. F., Olley J. M., Yoshida H., and Laslett G. M. (1999) Optical dating of single and multiple grains of quartz from Jinmium rock shelter (northern Australia); Part II, Results and implications. *Archaeometry* **41**, 365-395.

Rogalev B., Chernov V., Korjonen K., and Jungner H. (1999) Some features of IRSL in microcline from the Baikal region. *Radiation Protection Dosimetry* **84**, 461-466.

Rose J., Meng X. M., and Watson C. (1999) Palaeoclimate and palaeoenvironmental responses in the western Mediterranean over the last 140 ka: evidence from Mallorca, Spain. *Journal of the Geological Society* **156**, 435-448.

Sakurai T. and Gartia R. K. (1999) Analysis of the thermoluminescence glow curves of a brown microcline - effects of optical bleaching upon trap distribution. *Radiation Protection Dosimetry* **84**, 479-482.

Sanchez-Munoz L., Correcher V., Garcia-Guinea J., and Delgado A. (1999) Thermoluminescence of a lithium aluminium rich beta quartz for dosimetry purposes. *Radiation Protection Dosimetry* **84**, 543-546.

Schilles T., Lang A., Habermann J., and Rieser U. (1999) Improved single aliquot dating applications using a new highly efficient modular luminescence reader. *Radiation Protection Dosimetry* **84**, 363-366.

Shlukov A. I., Usova M. G., Voskovskaya L. T., and Shakhovets S. A. (1999) New absolute dating techniques for Quaternary sediments and their application on the Russian Plain. *GeoResearch Forum* **5**, 145-168.

Shulmeister J., Soons J. M., Berger G. W., Harper M., Holt S., Moar N., and Carter J. A. (1999) Environmental and sea-level changes on Banks Peninsula (Canterbury, New Zealand) through three glaciation-interglaciation cycles. *Palaeogeography, Palaeoclimatology, Palaeoecology* **152**, 101-127.

SiitariKauppi M., Pinnioja S., Kemppainen M., and Lindberg A. (1998) Correlation between the composition and irradiation-induced luminescence of feldspars. *Radiochemistry* **40**, 499-502.
Stokes S. (1999) Luminescence dating applications in geomorphological research. *Geomorphology* **29**, 153-171.

Sunta C. M., Feria A. W. E., Piters T. M., and Watanabe S. (1999) Limitation of peak fitting and peak shape methods for determination of activation energy of thermoluminescence glow peaks. *Radiation Measurements* **30**, 197-201.

Swezey C., Lancaster N., Kocurek G., Deynoux M., Blum M., Price D., and Pion J. C. (1999) Response of aeolian systems to Holocene climatic and hydrologic changes on the northern margin of the Sahara: a high-resolution record from the Chott Rharsa basin, Tunisia. *The Holocene* **9**, 141-147.

Thorne A., Grün R., Mortimer G., Spooner N. A., Simpson J. J., McCulloch M., Taylor L., and Curnoe D. (1999) Australia's oldest human remains: age of the Lake Mungo 3 skeleton. *Journal of Human Evolution* **36**, 591-612.

Vogel J. C., Wintle A. G., and Woodborne S. M. (1999) Luminescence dating of coastal sands: overcoming changes in environmental dose rate. *Journal of Archaeological Science* **26**, 729-733.

Wintle A. G. (1999) Optical dating in southern Africa. *South African Journal of Science* **95**, 181-186.